Anti-cooperativity in the two electron oxidation of the S118C disulfide dimer of azurin

Amsterdam, M.C. van; Ubbink, M.; Canters, G.W.

ELSEVIER

www.elsevier.com/locate/ica
Inorganica Chimica Acta 331 (2002) 296–302

Inorganica Chimica Acta

Anti-cooperativity in the two electron oxidation of the S118C disulfide dimer of azurin

Irene M.C. van Amsterdam, Marcellus Ubbink, Gerard W. Canters *

Gorlaeus Laboratories, Leiden Institute of Chemistry, Leiden University, PO Box 9502, 2300 RA Leiden, The Netherlands

Received 7 August 2001; accepted 13 December 2001

Dedicated to Professor A.G. Sykes

Abstract

We have constructed a disulfide dimer of S118C azurin, in which two copper centers are coupled through a relatively short covalent pathway, and studied its electron transfer properties. The dimer exhibits intriguing mechanistic properties. Due to the strain in the molecule, caused by the limited accessibility of Cys118, anti-cooperativity occurs in the two step oxidation of the dimer with a difference in redox potential between the two half reactions of 33 mV. Upon oxidation, the dimer favours the semi-reduced over the fully oxidized state, as the Cu(I) site in the semi-reduced dimer is able to stabilize the strained dimer complex. The internal electron transfer is surprisingly slow, which could be partially due to an increase in reorganization energy.

Keywords: S118C azurin dimer; Electron transfer; NMR spectroscopy; Strain; Redox potential

1. Introduction

Azurin is a well-characterized blue copper protein, which makes the protein highly suitable for studying the different factors that control long-range electron transfer. In partly oxidized solutions of azurin, electrons are transferred between reduced and oxidized molecules in a so-called electron self-exchange (e.s.e.) reaction. Although the structure of the binary complex in the e.s.e. reaction is unknown, NMR studies have shown that the hydrophobic patch surrounding the surface exposed copper ligand His117 is the site of interaction [1–4]. A clear demonstration of how the association of two molecules along this patch may occur, is provided by the crystal structure, where two water molecules connect the two His117 copper ligands via hydrogen bonds [5,6]. The water molecules are thought to be present also in the transient complex in solution and to enhance the electronic coupling, thus promoting the self-exchange reaction [7].

Recently, we have shown that water molecules in the protein interface help transferring electrons in covalently linked dimers of azurin [8,9]. In these studies we cross-linked two azurin monomers through cysteines that had been engineered in the hydrophobic patch at position 42, thereby replacing Asn42. It was found that for fast intramolecular electron transfer in the dimer, the partners in the complex require a specific orientation with the hydrophobic patches arranged opposite to each other. Crystallographic data show the presence of two water molecules in the protein interface, similar to the non-covalent wild type dimer complex [9].

Here we report on an extension of our electron transfer studies of azurin dimers. Again, we have constructed a dimer that is linked via the hydrophobic patch. However, in this case the solvent exposed serine 118 is replaced by a cysteine, thereby enabling the formation of disulfide linked dimers in which the two copper centers are coupled through a relatively short *covalent* pathway. Cys118 is positioned next to the copper coordinating ligand His117 and a path consisting of 19 covalent bonds (including the two Cu–N^{δ}(His117) bonds) connects the two coppers via the histidines 117 and cysteines 118 (see Fig. 1). Remarkably, the Cu sites demonstrate anti-cooperativity in

* Corresponding author. Tel.: +31-71-527 4256; fax: +31-71-527 4349.
E-mail address: canters@chem.leidenuniv.nl (G.W. Canters).

0020-1693/02/$ - see front matter
PII: S0020-1693(02)00688-6

their oxidation behavior, resulting in a redox potential difference for the first and second oxidation step of the dimer. In addition, the internal electron transfer rate is surprisingly slow.

2. Experimental

2.1. Protein preparation

The S118C azurin (*Pseudomonas aeruginosa*) mutant was constructed and isolated under reducing conditions in its apo-form as described previously, as were N42C and K27C azurin [8,10,11]. Dimers were formed in the presence of Cu(II). Typically, 1.1 molar equivalents of a $Cu(NO_3)_2$ solution and an excess (5 molar equivalents) of $K_3[Fe(CN)_6]$ were added to an apo-S118C azurin solution in 20 mM HEPES, pH 7, to obtain approximately 63% of the (Cu(II)–Cu(II))-dimer. Gel filtration chromatography was used to purify the S118C dimer from the monomeric form (Superdex 75 (Pharmacia), length, 60 cm; ∅, 1.6 cm; buffer: 20 mM HEPES, 150 mM NaCl, pH 7).

Protein NMR samples were typically 0.9 mM in total protein concentration in 99.9% deuterated 25 mM potassium phosphate buffer, pH* 8.5, prepared as described previously [8]. The pH was not corrected for the deuterium isotope effect, and is denoted as pH*. Reduced protein samples were obtained by incubation with one equivalent of ascorbic acid, which was subsequently removed by repeated concentration and dilution using an Amicon ultrafiltration cell. Argon was passed through all buffers and protein solutions prior to use to prevent re-oxidation. Partially oxidized samples were obtained by adding Cu(II) protein dimer to the reduced protein dimer, both taken from stock solutions of the same concentration. The concentration of oxidized azurin in the samples was measured with a special sample holder, that was designed to allow the absorbance of the protein solution to be measured around 628 nm in the NMR tube on a Perkin–Elmer lambda 18 spectrophotometer using optical fibers (Hellma, Müllheim/Baden, Germany). The percentage of oxidized azurin was measured relative to a fully oxidized sample before and after recording the NMR spectrum. The average of the two values was used in the analysis.

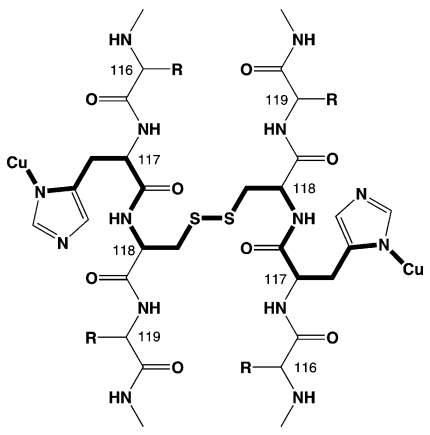

Fig. 1. Schematic representation of covalent electron transfer pathway from Cu to Cu (thick bonds) in disulfide linked S118C azurin dimer.

2.2. UV–Vis spectroscopy

UV–Vis spectra were recorded at 20 °C on a Shimadzu 2101PC and a Perkin–Elmer lambda 18 spectrophotometer. Samples were in 20 mM HEPES, pH 7 except for the NMR samples (vide supra).

2.3. NMR spectroscopy

^{1}H NMR spectra were acquired on a Bruker Avance DMX 600 MHz spectrometer at 313 K. The spectral width was 12.98 ppm. Free induction decays were accumulated in 16 K memory and Fourier-transformed using a squared sine window function. The chemical shifts were calibrated using sodium 3-(trimethylsilyl)propionate (TSP, 200 μM) as an internal reference.

2.4. Analysis

The resonance of the Val31 methyl group at -0.7 ppm was decomposed into a sum of peaks by using multiple peak fitting procedures and Lorentzian peak functions. The data was fitted with three components, which were assigned as RR (signal from fully reduced dimer), R(O) (signal from reduced half of semi-reduced dimer) and OO/(R)O (signals from fully oxidized dimer plus oxidized half of semi-reduced dimer). The peak positions and widths were kept constant with maximal error margins of 0.006 ppm and 3.0 Hz, respectively. From the peak areas the ratio between fully reduced (RR), semi-reduced (RO) and fully oxidized (OO) dimers was determined.

2.5. Redox potential

The redox properties of the S118C azurin dimers were studied by looking at the equilibrium reaction between reduced and oxidized azurin dimers:

$$\mathrm{RR} + \mathrm{OO} \underset{k_{-1}}{\overset{k_1}{\rightleftharpoons}} 2\mathrm{RO} \tag{1}$$

with the equilibrium constant:

$$K = \frac{k_1}{k_{-1}} = \frac{[\mathrm{RO}]^2}{[\mathrm{RR}]\cdot[\mathrm{OO}]} \tag{2}$$

The corresponding half-reactions with their potentials are:

$$RR \rightleftharpoons RO + e \qquad E_1 = E_1^0 + \frac{RT}{nF} \ln \frac{[RO]}{[RR]} \tag{3}$$

$$RO \rightleftharpoons OO + e \qquad E_2 = E_2^0 + \frac{RT}{nF} \ln \frac{[OO]}{[RO]} \tag{4}$$

When RR and RO are equally good reductors, $\Delta E^0 \equiv E_2^0 - E_1^0 = 0$, $k_1 = k_{-1}$ and $K = 1$. However, when the two half reactions exhibit different redox potentials, then $\Delta E^0 \neq 0$ and $k_1 \neq k_{-1}$. In that case the two step oxidation involves cooperativity ($\Delta E^0 < 0$; $k_1 < k_{-1}$) or anti-cooperativity ($\Delta E^0 > 0$; $k_1 > k_{-1}$), which will influence the relative concentrations of RR, RO and OO. The fractions of RR, RO and OO for each degree of oxidation (x) can be found as follows. As E_1 and E_2 (see Eqs. (3) and (4)) are equal to the solution potential, it follows that $E_1 = E_2$ and thus:

$$\Delta E^0 \equiv E_2^0 - E_1^0 = \frac{RT}{nF} \ln \frac{[RO]^2}{[RR]\cdot[OO]} \tag{5}$$

or

$$K = \frac{[RO]^2}{[RR]\cdot[OO]} = \exp(nF\Delta E^0/RT) \tag{6}$$

The total fraction of oxidized azurin (x) and reduced azurin ($1 - x$) can be expressed as:

$$x = \left([OO] + \frac{1}{2}[RO]\right)/[T] \tag{7}$$

$$1 - x = \left([RR] + \frac{1}{2}[RO]\right)/[T] \tag{8}$$

with:

$$[T] = [RR] + [RO] + [OO] \tag{9}$$

Substituting into Eq. (6) yields:

$$\frac{[RO]^2}{\left\{(1-x)[T] - \frac{1}{2}[RO]\right\}\cdot\left\{x[T] - \frac{1}{2}[RO]\right\}} = \exp(nF\Delta E^0/RT) \tag{10}$$

Eqs. (7)–(10) were used to fit the experimental fractions of RR, RO and OO from which ΔE^0 was obtained.

3. Results

3.1. Dimerization

Disulfide dimers of azurin were formed by the addition of $Cu(NO_3)_2$ to a solution of apo-azurin. Due to its participation in the disulfide formation, the copper becomes partially reduced, depending on the degree of dimerization. This was monitored by measuring the absorption around 628 nm, which is characteristic for the cysteine $S\pi \rightarrow Cu(II)$ $d(x^2 - y^2)$ transition in azurin [12,13]. When 1.1 molar equivalents of $Cu(NO_3)_2$ are added to the apo-azurin, a high degree of dimerization results in a relatively low absorbance at 628 nm. In the optical spectrum of K27C azurin, which was used as a control, almost no absorption is observed at 628 nm; for N42C azurin, which was used in previous studies [8,9], a twofold decrease in absorbance is observed relative to a fully oxidized sample. For S118C azurin, a smaller effect is observed (20–30% reduction in absorbance). The limited dimerization of S118C azurin is also demonstrated by gel filtration analysis. Upon addition of an equimolar amount of copper, K27C azurin is completely dimerized, N42C azurin is dimerized up to approximately 75%, whereas S118C azurin is dimerized for about 50%. Addition of a slight excess of $K_3[Fe(CN)_6]$ results, apart from completely re-oxidizing the copper, in the conversion of up to 100% of the monomers into dimers for N42C, and of only 63% for S118C.

3.2. NMR spectroscopy

The one-dimensional ^1H NMR spectra of N42C and K27C azurin dimers are very similar to the wild type azurin, except for some line-broadening (3–4 Hz) as a result of the larger rotational correlation time of the dimer. This indicates that no structural changes have occurred upon dimer formation in these two cases. The one-dimensional ^1H NMR spectrum of the S118C azurin dimer, however, shows several changes in resonance positions relative to the other dimers, indicating that structural rearrangements have occurred. In addition, a number of NMR peaks are relatively broad.

3.2.1. Redox potential difference

In order to determine the redox properties of the dimer we consider the proton resonance of the Val31 methyl group around -0.7 ppm in the NMR spectrum. This resonance is well resolved from other resonances and its chemical shift appears sensitive to the redox state of the protein [9,14]. In Fig. 2 (upper traces) this resonance is shown in the presence of varying percentages of oxidized protein, starting with a fully reduced form of the protein (peak at -0.68 ppm, bottom) to the fully oxidized species (peak at -0.74 ppm, top).

Upon oxidation, a peak appears at the resonance position of the fully oxidized protein (-0.74 ppm, Fig. 2). The intensity of this peak, as determined from multiple peak fitting, agrees with the measured percentage of oxidized protein (Fig. 3A), which is indicative for slow exchange. A second peak at -0.705 ppm, slightly shifted from the position of the fully reduced protein, comes up with increasing percentage of oxidized protein and disappears again when the oxidation approaches 100%. This can be clearly seen from the

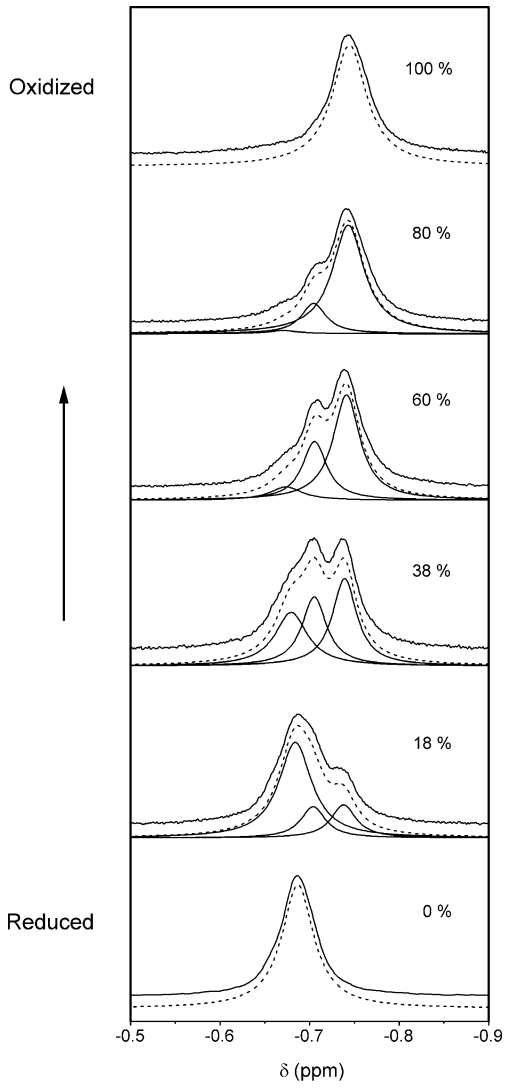

Fig. 2. Region of ^{1}H NMR spectrum of S118C azurin dimer at 600 MHz showing the Val31 methyl resonance around -0.7 ppm as a function of the percentage of oxidized protein present in the solution as indicated. The experimental data are shown in the upper traces (solid). The results from the peak analysis are offset for the sake of clarity and shown in solid (separate peaks) and dashed traces (sum of separate peaks).

peak analysis, presented in the traces underneath each experimental spectrum in Fig. 2. The intensities of the peak at -0.68 ppm (fully reduced species) and the peak at -0.705 ppm together correspond to the total amount of reduced protein as shown in Fig. 3A (dashed line). The positions of the resonances do not change as a function of the degree of oxidation, which again, points towards slow exchange. As mentioned above, we conclude that the resonance at -0.705 ppm originates from a reduced form of the protein. Evidently, upon partial oxidation of the RR form the Cu(II) in one monomer affects the other (Cu(I) containing) monomer, causing a shift of the Val31 methyl resonance of the latter. Thus, the peak at -0.705 ppm represents the resonance of the Val31 methyl group in the reduced part of the semi-reduced dimer (denoted as R(O) in Fig. 3A). On the other hand, the signal from the Cu(II) half of the semi-reduced dimer (denoted as (R)O) is insensitive to the state of oxidation of the other half, and coincides with the resonance of the fully oxidized protein at -0.74 ppm.

Based on these findings the experimental fractions of fully reduced (RR), semi-reduced (RO) and fully oxidized (OO) dimer could be derived from the experimental peak areas (Fig. 3A). The results are plotted in Fig. 3B and were fitted by using Eq. (7)–(10). From the best fit a redox potential difference between the first and second oxidation step of the dimer of $\Delta E^0 = 33 \pm 5$ mV was obtained, showing anti-cooperativity in the two step oxidation. For a comparison the calculated ratios between RR, RO and OO at $\Delta E^0 = 0$ are plotted in Fig. 3B as well (dashed lines).

3.2.2. Electron self-exchange rates

From the peak analysis of the NMR data it is clear that the inter- as well as the intramolecular electron

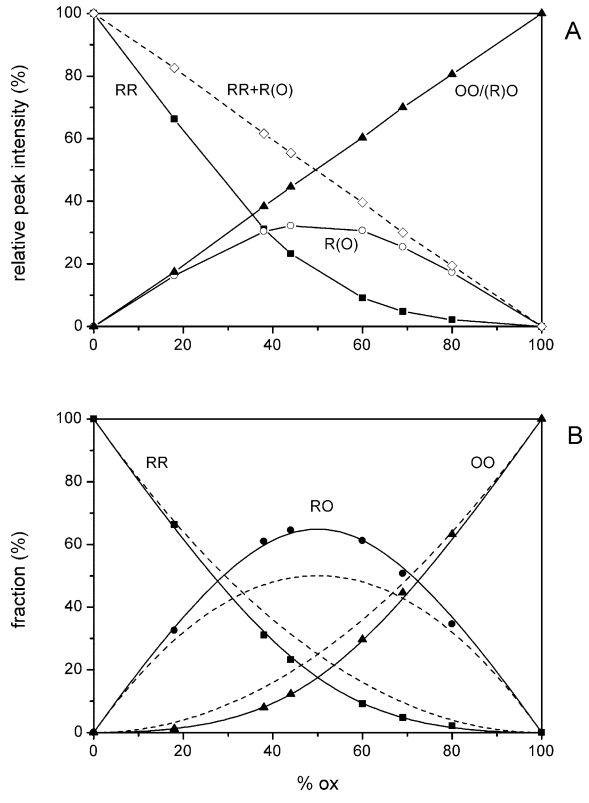

Fig. 3. Results from NMR peak analysis. (A) Relative peak intensities of RR (-0.68 ppm, ■), R(O) (-0.705 ppm, ○) and OO/(R)O (-0.74 ppm, ▲) as a function of the percentage of oxidized protein. Also the sum of RR and R(O) is indicated (dashed line, ◇). (B) Calculated fractions of RR (■), RO (●) and OO (▲) at different oxidation grades derived from Fig. 3A. The solid lines represent the least squared fit according to Eqs. (7)–(10) from which ΔE^0 of 33 mV was obtained. The dashed lines represent the calculated fractions of RR, RO and OO at $\Delta E^0 = 0$ mV.

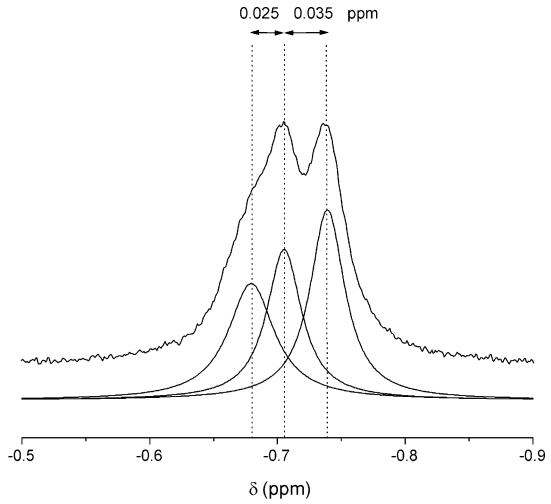

Fig. 4. Region of ^{1}H NMR spectrum of a 38% oxidized S118C azurin dimer clearly showing that the position of the peak at -0.705 ppm is not the average of the ones at -0.68 and -0.74 ppm.

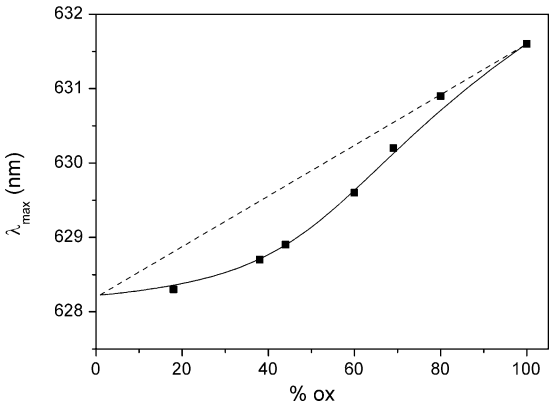

Fig. 5. λ_{max} as a function of the percentage of oxidized S118C azurin dimer fitted using Eq. (11). (solid line, $\Delta E^0 = 42$ mV). For a comparison λ_{max} at $\Delta E^0 = 0$ mV is shown as well (dashed line).

exchange must be slow. The peaks for the reduced and oxidized species are distinct and do not shift or broaden upon oxidation. The assignment of the peaks and their relative peak intensities correlate with the degree of oxidation. We emphasize that the resonance at -0.705 ppm cannot be assigned as an exchange peak resulting from fast intramolecular exchange between reduced and oxidized protein, since the position of this resonance is not the average of the resonance positions of the fully reduced and oxidized proteins (Fig. 4), unlike the situation in the BMME-linked N42C azurin dimer [9]. An upper limit for the intramolecular electron exchange rate can be obtained from the width of the resonance of R(O). The broadening of this resonance is less than 1 Hz resulting in an upper limit for the intramolecular electron transfer rate ≤ 3 s^{-1} [15].

An upper limit for the intermolecular electron exchange between two dimers of S118C azurin is obtained from the RR peak at 18% oxidation. The fitted data show < 1 Hz of line-broadening, which results in an upper limit for the intermolecular exchange rate of $\leq 10^4$ M^{-1} s^{-1}.

3.3. UV–Vis spectroscopy

The electronic spectrum of wild type azurin is characterized by a strong absorption at $\lambda_{max} = 628$ nm ($\varepsilon = 5.7$ mM^{-1} cm^{-1}) [1]. In the fully oxidized form of the S118C azurin dimer this transition occurs at a slightly different wavelength of $\lambda_{max} = 631.6$ nm with $\varepsilon = 4.9$ mM^{-1} cm^{-1} (per Cu-site)[1]. However, when lowering the degree of oxidation the absorption maximum gradually shifts back to $\lambda_{max} = 628.3$ nm (at 18% oxidation), as shown in Fig. 5. This remarkable feature is not present in other azurin dimers studied so far, and therefore, is specific for S118C azurin. The experimental data points were fitted by Eq. (11), which is based on the assumption that the peak position is a weighted average of the peak positions of the RO and OO species with an absorption maximum at λ_{max_RO} for the protein in its RO state, extinction coefficients per Cu-site of ε_{RO} and ε_{OO}, and in which the fractions RO and OO are defined by ΔE^0 (Eqs. (7)–(10)).

$$\lambda_{max} = \left(\lambda_{max\_RO}\frac{RO\cdot\varepsilon_{RO}}{RO\cdot\varepsilon_{RO} + 2\cdot OO\cdot\varepsilon_{OO}}\right) + \left(631.6\frac{2\cdot OO\cdot\varepsilon_{OO}}{RO\cdot\varepsilon_{RO} + 2\cdot OO\cdot\varepsilon_{OO}}\right) \quad (11)$$

Fitting with $\varepsilon_{RO} = 5.7$ mM^{-1} cm^{-1} and $\varepsilon_{OO} = 4.9$ mM^{-1} cm^{-1} resulted in $\lambda_{max\_RO} = 628.2 \pm 0.1$ nm and $\Delta E^0 = 42 \pm 11$ mV (Fig. 5), which is in agreement with ΔE^0 as obtained from the NMR analysis (33 ± 5 mV).

4. Discussion

4.1. Strain

4.1.1. Dimer formation

To create an azurin dimer, with a relatively short *covalent* pathway between the active sites we have constructed the disulfide dimer of S118C azurin and analyzed its mechanistic properties. Although Cys118 is a solvent exposed residue, reaction of apo-S118C azurin with $Cu(NO_3)_2$ in the presence of $K_3[Fe(CN)_6]$ did not result in complete dimerization, in contrast to N42C and K27C azurin. Apparently, dimer formation is hindered because Cys118 is not as exposed as Cys42 and Cys27 are in N42C and K27C azurin, respectively.

[1] The extinction coefficient of the fully oxidized S118C azurin dimer is estimated based on the A_{631}/A_{280} ratio with $\varepsilon_{280} = 9.8$ mM^{-1} cm^{-1} [1].

From the structure of wild type azurin, in which a cysteine residue has been modeled at position 118, one can estimate that the surface accessible area of this cysteine is approximately 22 Å^2 [16]. For Cys42, and Cys27, these numbers are 85 and 111 Å^2, respectively. Furthermore, Cys118 is positioned relatively close to the α-helix in azurin, which further limits the accessibility of Cys118. We conclude that dimer formation is sterically hindered and that the Cys118 azurin monomers get slightly deformed upon dimer formation. The changes in the resonance positions in the NMR spectrum of the S118C azurin dimer relative to the other dimers also indicate that structural deformations have occurred upon dimerization.

4.1.2. Redox potential difference

By analyzing the changes in the position and composition of the Val31 resonance in the NMR spectrum of the S118C azurin dimer with increasing oxidation (Fig. 2) the following striking features were observed. First, the Cu(I) half of the RO dimer appears to be influenced by the Cu(II) half of the dimer causing a shift in resonance position relative to the RR dimer. Such an effect has not been observed in other azurin dimers. Presumably, a small change in the geometry of the reduced copper site occurs when the other site becomes oxidized, which is not surprising as the link is close to the His117 Cu ligand.

Second, the NMR results show that the difference in the redox potential between the first and second oxidation step is 33 ± 5 mV, which leads to $K = k_1/k_{-1} = 3.4$ at $T = 313$ K (see Eqs. (2) and (6)). Thus, the dimer has a preference to be semi-reduced (RO). Too much strain in the molecule destabilizes the dimer with two oxidized copper sites. Apparently, the oxidation of the second copper site cannot be compensated by a change in geometry of the site that is already oxidized. Further support for these conclusions comes from optical spectroscopy. The optical data clearly show that the S118C dimer in its fully oxidized state exhibits an absorption maximum at a different wavelength than the dimer in its RO state (Fig. 5). We conclude that the dimer in its fully oxidized (OO) state needs to adjust the geometry of its Cu(II) site(s) relative to the Cu(II) site in the RO state. This change in geometry is accompanied by a decrease in extinction coefficient (per Cu-site) of OO relative to RO. The redox potential difference of 42 ± 11 mV obtained from fitting the optical data confirms the results as found from the NMR analysis. An EPR study of a possible geometry change is in progress.

4.2. Electron self exchange rates

The NMR experiments show that the electron exchange within and between S118C azurin dimers is slow. Upper limits for the intra- and intermolecular e.s.e were determined as 3 s^{-1} and 10^4 M^{-1} s^{-1}, respectively.

Regarding intramolecular long-range electron transfer, the theory predicts that the electronic coupling H_{AB} and consequently the electron transfer rate (k_{ET}) decrease approximately exponentially with increasing distance between donor and acceptor. This is reflected by Eq. (12), which represents a simplified form of the Marcus equation [17]:

$$k_{ET} = k_0 \cdot \exp[-\beta(r - r_0)] \cdot \exp[-(\Delta G^0 + \lambda)^2/4\lambda k_B T] \quad (12)$$

k_0 (ca. 10^{13} s^{-1}) is the rate constant for donors and acceptors that are in van der Waals contact, r represents the donor-acceptor distance, whereas r_0 is the close contact distance. β is a parameter reflecting the efficiency of the protein medium to mediate electron transfer. ΔG^0 and λ represent the free energy and reorganization energy, respectively. In the so-called tunneling pathway model of Beratan and Onuchic, the electronic coupling H_{AB} is specified as the product of the individual connections, which can be covalent bonds, hydrogen bonds or through space jumps [18]:

$$H_{AB}^2 = (H_{AB}^0)^2 \cdot \exp[-\beta(r - r_0)] = (H_{AB}^0)^2 \cdot f_M^2 \quad (13)$$

where f_M represents a dimensionless decay factor [19]. Following the pathway via 19 covalent bonds from Cu to Cu via the His117 and Cys118 residues within the S118C azurin dimer (Fig. 1) the electronic coupling decay for S118C dimer is calculated as 6.1×10^{-5} ($= f_M$). For comparison, the calculated electronic coupling decay for the N42C dimer involving six covalent bonds and three hydrogen bonds is 1.1×10^{-3}, which differs by a factor of 20. When applying Eq. (12) with $k_0 = 10^{13}$ s^{-1}, $T = 313$ K, $\Delta G^0 = 0$ eV (e.s.e. reaction) and $\lambda = 0.7$ eV [20] in combination with the tunneling pathway model (substituting the squared decay factor, f_M^2, for ($\exp[-\beta(r - r_0)]$), Eqs. (12) and (13)), the calculated intramolecular electron transfer rate is 0.6×10^2 s^{-1}. From our experimental data an upper limit for the intramolecular electron transfer rate within the S118C dimer is determined as ≤ 3 s^{-1}, which is roughly an order of magnitude lower. This relatively low value could be due to a reorganization energy that is somewhat larger than 0.7 eV. Due to the strain in the molecule both copper centers need to adjust their geometry upon exchange of an electron. Alternatively, the nature of the Cu–N bond could be taken into consideration. In the calculation of the f_M factor the Cu–N bond was given the same decay value as a covalent C–C bond, but the relatively poor overlap between the His and Cu orbitals might correspond to a lower decay factor reducing the intramolecular electron transfer rate to a value less than 0.6×10^2 s^{-1}.

The bimolecular electron transfer rate of $< 10^4$ M^{-1} s^{-1} between the two molecules of S118C azurin dimer is also slow, as compared with wild type azurin ($\sim 10^6$

M^{-1} s^{-1}). The hydrophobic patch surrounding His117 has been shown to be the site of interaction for intermolecular electron transfer [1–4]. As a result of the dimerization this patch is expected to be no longer exposed to the solvent and, thus, to have become inaccessible for other dimers to form association complexes.

5. Conclusion

From an investigation of the electron exchange properties in S118C disulfide dimers it was found that the dimer exhibits a relatively low intramolecular electron exchange rate (≤ 3 s^{-1}). For the intermolecular electron transfer rate an upper limit of 10^4 M^{-1} s^{-1} was determined. In addition to these results we have observed that the S118C dimer exhibits very intriguing characteristics. The formation of dimers appears to be impeded by structural constraints causing slight structural deformation of the monomers. Upon oxidation the dimer favours the semi-reduced state over the fully oxidized state due to strain within the molecule. This is shown by the difference in redox potential between the redox couples RR/RO and RO/OO of approximately 33 mV. Presumably, when the protein is converted from its fully reduced to its semi-reduced state, the Cu(I) site is slightly distorted by the more rigid Cu(II) site, which is reflected in a shift of the Val31 resonance in the NMR spectrum. Compensation by changing the geometry of the copper site of the counterpart is not possible when the protein is in its fully oxidized state and, therefore, the presence of two oxidized coppers in one dimer is not favored. These conclusions indicate that an increase in reorganization energy is a likely cause for the relatively low intramolecular electron exchange rate. The present findings are in line with the results of a spectroscopic and mechanistic study of the His117Gly azurin variant from which it was concluded that the Cu-ligand interaction is weakened upon the reduction of the Cu site [21]. A remarkable conclusion of the present work is that structural fluctuations of the size of thermal fluctuations may give rise to substantial variations in redox potential. This is also relevant for studies in which proteins are immobilized on a solid substrate. As the immobilization often gives rise to small distortions in protein structure it does not need to surprise that the redox potential measured for instance by CV sometimes deviates from the potential determined for the protein free in solution.

Acknowledgements

The authors would like to use this opportunity to express their appreciation for the many contributions of Professor Sykes to the field of Bioinorganic Chemistry.

References

[1] M. van de Kamp, M.C. Silvestrini, M. Brunori, J. van Beeumen, F.C. Hali, G.W. Canters, Eur. J. Biochem. 194 (1990) 109.
[2] M. van de Kamp, R. Floris, F.C. Hali, G.W. Canters, J. Am. Chem. Soc. 112 (1990) 907.
[3] M. van de Kamp, G.W. Canters, C.R. Andrew, J. Sanders-Loehr, C.J. Bender, J. Peisach, Eur. J. Biochem. 218 (1993) 229.
[4] G. van Pouderoyen, S. Mazumdar, N.I. Hunt, H.A.O. Hill, G.W. Canters, Eur. J. Biochem. 222 (1994) 583.
[5] H. Nar, A. Messerschmidt, R. Huber, M. van de Kamp, G.W. Canters, J. Mol. Biol. 221 (1991) 765.
[6] H. Nar, A. Messerschmidt, R. Huber, M. van de Kamp, G.W. Canters, J. Mol. Biol. 218 (1991) 427.
[7] K.V. Mikkelsen, L.K. Skov, H. Nar, O. Farver, Proc. Natl. Acad. Sci. USA 90 (1993) 5443.
[8] I.M.C. van Amsterdam, M. Ubbink, L.J.C. Jeuken, M.Ph. Verbeet, O. Einsle, A. Messerschmidt, G.W. Canters, Chem. Eur. J. 7 (2001) 2398.
[9] I.M.C. van Amsterdam, M. Ubbink, O. Einsle, A. Messerschmidt, A. Merli, D. Cavazzini, G.L. Rossi, G.W. Canters, Nat. Struct. Biol. (2001) 9 (2002) 48.
[10] J.J. Davis, C.M. Halliwell, H.A.O. Hill, G.W. Canters, M.C. van Amsterdam, M.Ph. Verbeet, New J. Chem. 22 (1998) 1119.
[11] M. van de Kamp, F.C. Hali, N. Rosato, A. Finazzi-Agro, G.W. Canters, Biochim. Biophys. Acta 1019 (1990) 283.
[12] K. Pierloot, J.O.A. de Kerpel, U. Ryde, M.H.M. Olsson, B.O. Roos, J. Am. Chem. Soc. 120 (1998) 13156.
[13] E.I. Solomon, K.W. Penfield, A.A. Gewirth, M.D. Lowery, S.E. Shadle, J.A. Guckert, L.B. LaCroix, Inorg. Chim. Acta 243 (1996) 67.
[14] G.W. Canters, H.A.O. Hill, N.A. Kitchen, E.T. Adman, J. Magn. Reson. 57 (1984) 1.
[15] P.J. Hore, Nuclear Magnetic Resonance, Oxford University Press, Oxford, UK, 1995, p. 44.
[16] S.J. Hubbard, J.M. Thornton, NACCESS Computer Program, Department of Biochemistry and Molecular Biology, University College, London, 1993.
[17] R.A. Marcus, N. Sutin, Biochim. Biophys. Acta 811 (1985) 265.
[18] D.N. Beratan, J.N. Onuchic, in: D.S. Bendall (Ed.), Biological Electron Transfer, Bios Scientific Publishers, Oxford, UK, 1996, p. 23.
[19] G.W. Canters, M. van de Kamp, Curr. Opin. Struct. Biol. 2 (1992) 859.
[20] H.B. Gray, B.G. Malmström, R.J.P. Williams, J. Biol. Inorg. Chem. 5 (2000) 551.
[21] L.J.C. Jeuken, M. Ubbink, J.H. Bitter, P. van Vliet, W. Meyer-Klaucke, G.W. Canters, J. Mol. Biol. 299 (2000) 737.